



Research Paper

IGDT-Based Epsilon-Constraint Multi-Objective Optimal Planning of Hybrid Ship Power System with Renewable Energy Resources and Energy Storage System

Mohammad Alizadeh Golmahalleh^{1,*}  and Meysam Jafari-Nokandi² 

¹Faculty of Electrical and Computer Engineering, Imam Khomeini Naval University, Nowshahr, Iran.

²Faculty of Electrical and Computer Engineering, Babol Noshirvani University of Technology, Babol, Iran.

Abstract— The integration of solar generation and Energy Storage Systems (ESSs) into ship power systems has gained increasing attention. This trend is primarily driven by stringent Marine Pollution Protocol regulations and the increasing integration of Renewable Energy Sources (RESs). Integrating RESs and BESSs into ship power systems helps reduce pollutant emissions from fossil fuel generators. However, inadequate sizing of hybrid ship power systems may result in high investment costs and elevated greenhouse gas emissions. This article introduces a Mixed-Integer Linear Programming model for identifying the optimal configuration of RESs and BESSs. The model incorporates two objective functions, aiming to minimize both costs and pollutant emissions. In the proposed model, the possibility of using four different technologies -lead-acid, nickel-cadmium, lithium-ion, and sodium-sulfur- has been considered for BESSs. For optimal energy management of a hybrid ship power system under photovoltaic radiation uncertainty along the route, Information Gap Decision Theory has been utilized. Considering the two contradictory objective functions in the proposed model, the ϵ -constraint method has been used to determine Pareto optimal responses, and the fuzzy inference method has been used to determine the final optimal response. The proposed model has been evaluated through four distinct case studies. The analysis of the results shows that using the optimal sizing of RESs and BESSs can lead to a simultaneous reduction in costs and emissions.

Keywords—Hybrid ship power system planning, information gap decision theory, epsilon constraint.

NOMENCLATURE

Indices and Sets

| | |
|----------|--|
| Γ | Set of uncertain parameters |
| d | Index of battery depth of discharge segments |
| g | Index of generators |
| i | Index of ESS technology |
| o | Index of discretization |
| s | Index of seasons |
| t | Index of time intervals |

Parameters

| | |
|-----------------------------|---|
| ΔG | Discretization step of the variable G_{pv} |
| $\eta_i^{ch}, \eta_i^{dch}$ | Charging/discharging efficiency for battery i |
| a | Interest rate [%] |
| C_{CSU}^g | Cold startup cost for diesel generator g |
| C_{HSU}^g | Hot startup cost for diesel generator |
| C_{cap}^{PV} | Capital cost of PV |
| C_{rep}^{PV} | Replacement cost of PV |
| CE_i^{ESS} | BESS energy investment cost [\$/kWh] |

| | |
|------------------------|---|
| CI_i^{ESS} | BESS installation cost [\$/kWh] |
| CO_i^{ESS} | BESS operation and maintenance cost [\$/kW/year] |
| CP_i^{ESS} | BESS power investment cost [\$/kW] |
| $G_{t,s}^{PV}$ | Hourly solar irradiance (W/m ²) |
| mut, mdt | Minimum/maximum time each generator is allowed to be on/off |
| N_i^{max} | Number of life cycles of battery i at maximum DoD |
| O | Number of discretization for variable G_{pv} |
| P_g^{min}, P_g^{max} | Minimum/maximum active power limit of diesel generator g |
| $P_{t,s}^D$ | Active load at time t and season s |
| R_{max} | Maximum rate of change of production power of generators |
| TL | Planning lifetime (year) |
| η^{PV} | PV panels efficiency |
| $\xi_{i,d}$ | Maximum depth of discharge (DoD) of BESS |
| A^{PV} | Each PV panel area (m ²) |
| $N_{i,d}$ | Number of life cycles of battery i at DoD d |

Variables

| | |
|-------------------------|--|
| α | Maximum possible deviation of predicted uncertainty parameter from its predicted value |
| $\delta_{g,t,s}^{cold}$ | Binary variable indicating cold startup status of generator g at time t and season s |
| $\delta_{g,t,s}^{hot}$ | Binary variable indicating hot startup status of generator g at time t |
| $\delta_{g,t,s}^{SU}$ | Binary variable indicating startup status of generator g at time t and season s |
| $\delta_{g,t}^{SD}$ | Binary variable indicating shutdown status of generator g at time t |

Received: 04 Feb. 2025

Revised: 06 Apr. 2025

Accepted: 04 Jun. 2025

*Corresponding author:

E-mail: golmahalleh63@gmail.com (M. Alizadeh Golmahalleh)

DOI: 10.22098/joape.2025.16711.2290

This work is licensed under a [Creative Commons Attribution-NonCommercial 4.0 International License](https://creativecommons.org/licenses/by-nc/4.0/).

Copyright © 2025 University of Mohaghegh Ardabili.

| | |
|----------------------------|---|
| $\psi_{i,t,s}^B$ | Binary variable indicating lifecycle of battery i |
| $C_{g,t,s}^{fuel}$ | Fuel consumption cost of diesel generator g at time t and season s |
| $C_{g,t,s}^{SU}$ | Startup cost for diesel generator g at time t and season s |
| $Cost_{DG}$ | Diesel generator cost (\$) |
| $Cost_{ESS}$ | ESS cost (\$) |
| $Cost_{PV}$ | PV cost (\$) |
| E_i^B, P_i^B | Battery rated energy and rated power |
| OF_j^{\min}, OF_j^{\max} | Minimum/maximum of objective function j |
| OF_j | Value of objective function j |
| $P_{t,s}^{PV-used}$ | Hourly used PV power |
| $P_{t,s}^{PV}$ | Total power of generated PV system |
| $Pch_{i,t,s}^B$ | Charging power of battery i at time t and season s |
| $Pdch_{i,t,s}^B$ | Discharging power of battery i at time t and season s |
| $p_{Ct,s,o}$ | Power corrections for linearization of two real variables |
| $SOC_{i,t,s}$ | State of charge of battery i at time t and season s |
| $v_{i,t}, w_{i,t}$ | Binary variable indicating on/off status of generator i |
| $Z_{i,t,s}^B$ | Binary variable representing charging status of battery i at time t in season s |
| $\mu_j(x)$ | Value of objective function j in Pareto response x |
| $\omega_{i,d}$ | Binary variable indicating selected maximum DoD for battery i |
| P^{ins} | Total power of installed PV system |
| $P_{g,t,s}$ | Active power generation of diesel generator g at time t and season s |
| $U_{g,t,s}$ | Binary variable indicating status of generator g at time t and season s |
| W_j | Weighting coefficients of objective function j |
| $x_{t,s,o}$ | Binary variables indicating the range of real variable G_{PV} |

1. INTRODUCTION

The growing awareness of the consequences of global warming, which stem from air pollution and the depletion of fossil fuels, has generated significant interest and opened up opportunities within the transportation sector, especially in the maritime industry. Reports from the International Maritime Organization (IMO) indicate that marine transportation was responsible for 2.2% of global CO_2 emissions in 2012, with projections suggesting a potential increase of 50% to 250% by 2050 if no action is taken. As a result, the IMO has mandated the shipbuilding industry to enhance the effectiveness of onboard energy systems to mitigate CO_2 emissions [1–3]. Within this context, the integrated power system technology has emerged as an appealing alternative to conventional ships, as it employs all-electric ship configurations that integrate electric propulsion with a ship service electric grid, providing a unified electrical platform. photovoltaic (PV) technology and ESS garnered significant interest within the scientific community a few years ago and were the subject of experimental research. However, the considerable investment cost associated with PV and ESS hindered its widespread adoption in the maritime domain. Recently, with rising oil prices and decreasing PV and ESS investment costs, many ships have opted to incorporate these technologies. The objective of this trend is to reduce greenhouse gas emissions, improve energy efficiency, and attain cost savings in operations.

To reduce the fuel costs and pollution emissions in ships, different kinds of renewable resources and ESS can be used in power systems. In the articles, numerous approaches have been suggested to ascertain the optimal sizing of renewable resources and ESS. A review and analysis of Hybrid ESS in renewable energy, discussing their significance, current state, trends, and comparisons with other energy storage systems have been made in [4]. For a shipboard power system, reference [5] analyzes the techno-economic performance, covering technical, emissions, and economic aspects, of three distinct hybrid systems including PV/fuel cell/wind/battery/diesel generators and feature two different battery technologies: lithium-ion and lead-acid. In

[6], a stochastic programming approach has been presented for determining the optimal sizing of a hybrid ship power system, which incorporates an ESS, PV panels, and a diesel generator. This method considers the uncertainty associated with the hourly global solar irradiation and its impact on the PV system's output power. In [7], the optimization of the PV system and BESS sizes has been conducted using the weighted sum method. The objective of this optimization is to simultaneously reduce the annual cost and pollution emissions. A microgrid with a solar PV system and multiple storage components has been analyzed in [8], aiming to optimally size the PV plant, battery, fuel cell, electrolyzer, and hydrogen tank to meet load demand while minimizing life cycle cost. To address PV and load uncertainties, a chance-constrained Mixed-Integer Linear Programming (MILP) model is formulated for optimal sizing. A study in [9] has introduced a mixed-integer quadratic programming model for determining the optimal capacity of an ESS for a marine ferry ship. This approach involves simultaneous optimization of ESS sizing and power system scheduling. The optimal management of ESS in conjunction with distributed generators can yield several benefits [10, 11]. These include peak load shaving, reducing the need for costly power system upgrades, and mitigating negative environmental impacts. By efficiently utilizing ESS alongside distributed generation, power systems can achieve more efficient operation, cost savings, and improved sustainability. The effectiveness of ESS in enhancing the reliability and power quality of power systems has been highlighted [12–14]. Furthermore, ESS has been shown to facilitate the integration and increased penetration of distributed generation resources. In [15], some algorithms have been introduced for achieving the optimal sizing and management of ESSs integrated into existing shipboard power systems. The primary objective of this approach is to minimize fuel oil consumption, greenhouse gas emissions, and management costs associated with the power generation system. In [16], a methodology has been developed to calculate the optimal sizes of the ESS, PV, and diesel generators in a ship power system. The objective of this methodology is to minimize CO_2 emissions, fuel costs, and investment costs. In [17], a simulation model has been introduced that depicts the operation of a wind /PV/diesel hybrid power system with battery bank storage. The primary objective of this model is to minimize the cost of energy supplied by the system while simultaneously enhancing its reliability and efficiency. Reference [18] offers an extensive and comprehensive review that thoroughly investigates energy management techniques and their integration with ESS sizing. The focus is on predictive-based energy management strategies, including Reinforcement Learning, Artificial Neural Network, and Model Predictive Control. A MILP has been utilized in [19] to optimize the size of a hybrid renewable power system, considering PV cells, BESS, and FC to minimize energy costs and maximize profits from chemical products generated by seawater electrolysis, integrating advanced direct load control and rooftop PV generation. A novel probabilistic MILP formulation has been presented in [20] to optimize the capacity and type of renewable sources and ESS for minimizing energy costs associated with an FC System. The formulation considers FC performance requirements to achieve cost-effective operation while meeting the system's performance needs. In [21], a method has been proposed for determining the optimal sizing of a ship's power system. The focus is on optimizing the size of the diesel generator, the PV generation sources, and the ESS to minimize three key factors: investment cost, fuel cost, and CO_2 emissions.

The solar power generation in a sailing ship is influenced by various factors such as the time zone, local time, date, latitude, and longitude along the ship's navigation route. These variables affect the availability and intensity of sunlight, which directly impacts the amount of power generated by the ship's PV system. In [6], a method has been developed to correct the output of PV modules by considering the seasonal and geographical variations of solar irradiation and temperatures along

a route. A universal mathematical model has been formulated in [22] to describe PV power generation on ships, taking into account sea conditions and integrated ship motion, and analyzes the fluctuation characteristics of PV output power, providing insights for optimizing PV system design and operation in marine environments. The exploration of optimization models with multiple objectives has been a significant area of research, with numerous papers contributing to the development and refinement of approaches to solve these complex problems. Reference [23] presents a study on designing a reliable and optimal hybrid renewable energy system. The study utilizes the epsilon-constraint method and a coyote optimization algorithm to determine optimal component sizing. Objectives include minimizing loss of load probability, CO_2 emissions, and the system's annualized cost. In [24], a multi-objective bi-level optimization approach has been proposed for component sizing and energy management, utilizing a particle swarm optimization algorithm and an adaptive equivalent consumption minimization strategy. A multi-objective optimization method has been proposed in [25] to optimize hybrid ESS sizing and EMS design simultaneously using support vector machine and frequency control techniques. Reference [26] introduces a novel method for determining the optimal size of an ESS by minimizing fuel cost, investment/replacement cost, and CO_2 emissions. The approach considers the ESS lifespan and employs a clustering algorithm to handle high-dimensional uncertain data. A double-loop optimization approach for ESS sizing and power allocation has been proposed in [27], integrating a battery degradation model with PSO-GWO optimization.

To the best of the authors' knowledge, no research paper has analyzed different BESS technologies to improve the performance of a ship hybrid power system, so this paper presents a comprehensive MILP model to determine the optimal sizing of a hybrid PV/diesel generator/ESS in a standalone ship power system considering different BESS technologies. The proposed model accounts for a wide range of technical and operational characteristics of BESS technologies and allows for selecting the optimal combination of technologies. In this article, the epsilon-constraint method has been used to determine the Pareto front while the fuzzy inference method has been employed to determine the optimal solution for solving the multi-objective optimization problem. Also, the Information Gap Decision Theory (IGDT) strategy has been used to make a robust decision against the uncertainty of solar radiation.

The rest of this paper is organized as follows: The proposed model is comprehensively formulated in section 2. The model is implemented on a ship power system in section 3 and the results are analyzed. Future studies are outlined in Section 4. Finally, the conclusion is given in section 5.

2. MATHEMATICAL MODEL OF HYBRID SHIP POWER SYSTEM

In this study, an analysis is conducted on the cost and emissions of a hybrid PV/diesel/ESS ship power system, as depicted in Fig. 1. The system configuration includes a PV array, two diesel generators for primary power generation, and a BESS to store surplus energy and enhance system reliability. The objective of this analysis is to assess the economic and environmental aspects of the hybrid power system. It considers factors such as the initial cost of the components, fuel consumption of the diesel generators, and the reduction in emissions achieved through the integration of the PV and ESS components. By evaluating the cost and emissions of this hybrid system, valuable insights can be gained regarding its feasibility, economic viability, and environmental benefits compared to conventional power systems used in ships [21].

2.1. Uncertainty modeling

Numerous models have been developed to address the uncertainties that currently exist. Multiple techniques have been

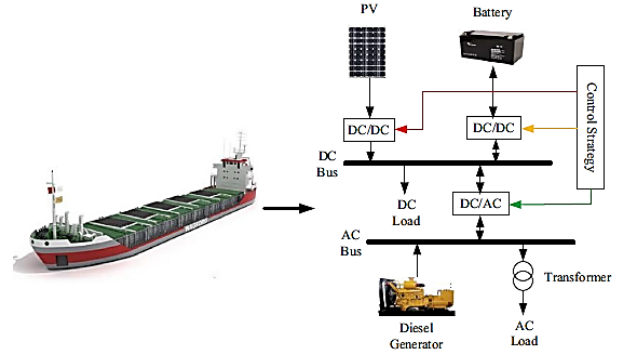


Fig. 1. Hybrid ship power system [21].

employed in power system analyses to represent uncertainty, encompassing probabilistic, hybrid, IGDT, and robust optimization methods. The research conducted in this study uses the IGDT technique to explore the impact of uncertainty on both the research hypothesis and the model. The IGDT method is a decision-making approach designed to maximize the robustness of a system when confronted with significant uncertainties.

To engage in risk-averse decision-making, it is necessary to acquire a set of decision variables that effectively enhance the objective function in response to deviations from the predicted value of the uncertain parameter. The decision-maker seeks assurance that the objective function's value will remain within the prescribed uncertainty radius. To assess the impact of uncertainty using the IGDT method, it is crucial to obtain the solution in a base case based on the predicted values of input parameters. Subsequently, the second level of optimization can adopt diverse decision-making strategies.

2.2. Objective function

In the proposed model and according to Eq. (1), the simultaneous minimization of two objective functions of investment and operating costs of the ship's power system and emission of pollutants from the diesel generators is considered. Eq. (2) shows the cost objective function, which includes diesel generator cost, PV investment cost, and battery investment cost, respectively.

$$Obj = \min \quad Cost \quad (1)$$

$$Cost = Cost^{DG} + Cost^{PV} + Cost^{ESS} \quad (2)$$

The energy production cost of diesel generators, which incorporates the fuel cost and the start-up cost, is represented by Eq. (3).

$$Cost^{DG} = \sum_{g=1}^G \sum_{t=1}^T \sum_{s=1}^S \left(C_{g,t,s}^{fuel} + C_{g,t,s}^{SU} \right) \quad (3)$$

The fuel cost of the generator is expressed in Eq. (4) as a quadratic function of the power output of that generator [9, 28, 29]:

$$C_{g,t,s}^{fuel} = a_g P_{g,t,s}^2 + b_g P_{g,t,s} + c_g \quad (4)$$

The relationships related to the start-up cost of diesel generators are given in Eqs. (5) and (6).

$$\delta_{g,t,s}^{SU} = \delta_{g,t,s}^{cold} + \delta_{g,t,s}^{hot} \quad (5)$$

$$U_{g,t,s} - \sum_{h=t-t_g^{cold}}^{t-1} U_{g,h,s} \leq \delta_{g,t,s}^{cold} \quad (6)$$

$$C_{g,t,s}^{SU} = \delta_{g,t,s}^{cold} \cdot C_g^{CSU} + \delta_{g,t,s}^{hot} \cdot C_g^{HSU} \quad (7)$$

To calculate the start-up cost, one of the two hot and cold start-up modes is considered based on the duration that a thermal unit has remained in the off state before being turned on. Equation Eq. (5) demonstrates that during the start-up process, either the hot or cold start-up mode can occur. According to Eq. (6), if the generator shutdown time is longer than a specific time, the generator should be started in a cold state. The determination of the generator start-up cost is achieved in Eq. (7) by specifying whether it is a cold or hot start-up.

The cost of BESS, which includes power and energy rating capital costs, installation costs, and operation and maintenance costs is stated in Eq. (8) [20].

$$Cost^{ESS} = \sum_i P_i^{ESS} (CRF \cdot CP_i^{ESS} + CO_i^{ESS}) + E_i^{ESS} \cdot CRF \cdot (CE_i^{ESS} + CI_i^{ESS}) \quad (8)$$

To convert the capital cost of the hybrid PV/diesel/ESS ship power system into an annual cost, the capital recovery factor (CRF), defined by Eq. (9), is utilized:

$$CRF = \frac{a(1+a)^{TL}}{(1+a)^{TL} - 1} \quad (9)$$

The installation and operating cost of the PV system is given in Eq. (10).

$$Cost^{PV} = CRF \cdot P^{ins} (C_{capital}^{PV} + C_{replacement}^{PV}) \quad (10)$$

The emission of pollutants from diesel generators as the 2nd objective function is stated in Eq. (11). Emission of pollutants is usually expressed as a quadratic function of the production power of thermal units [9, 30].

$$Emission = \sum_g \sum_t \alpha_g P_{g,t,s}^2 + \beta_g P_{g,t,s} + \gamma_g \quad (11)$$

It should be noted that reference [31] is used to linearize the quadratic function of Eqs. (4) and (11).

2.3. Constraints

The equality of produced and consumed electric power is expressed in Eq. (12).

$$\sum_{g=1}^{N_G} P_{g,t,s} + P_{t,s}^{PV-used} + \sum_i Pch_{i,t,s}^B = P_t^D + \sum_i Pdch_{i,t,s}^B \quad \forall t, s \quad (12)$$

The installed PV system power generation equations are given in Eqs. (13) and (14).

$$P_{t,s}^{PV} = P^{ins} \cdot G_{t,s}^{PV} \cdot \eta^{PV} \quad (13)$$

$$\begin{aligned} P_{t,s}^{PV-used} &\leq P_{t,s}^{PV} \\ P^{ins} &\leq A_{deck} \cdot P^{PV-rate} \end{aligned} \quad (14)$$

Eq. (13) determines the total solar production power according to the installation area of solar panels on the ship's deck and

hourly solar radiance (W/m^2). According to Eq. (14), the amount of solar power utilized per hour is constrained to be lower than the maximum capacity of the ship's solar production. The limitations related to the generation power of the diesel generator are expressed in Eqs. (15) to (20).

$$U_{g,t} \cdot P_g^{\min} \leq P_{g,t,s} \leq U_{g,t} \cdot P_g^{\max} \quad \forall g, t \quad (15)$$

$$|P_{g,t,s} - P_{g,t-1,s}| \leq R^{\max} \quad \forall g, t \quad (16)$$

$$U_{g,t,s} - U_{g,t-1,s} \leq \delta_{g,t,s}^{SU} \quad \forall g, t \quad (17)$$

$$\begin{aligned} U_{g,t,s} - U_{g,t-1,s} &= \\ \delta_{g,t,s}^{SU} - \delta_{g,t,s}^{SD} &\quad \forall g, t, s \end{aligned} \quad (18)$$

$$\sum_{h=t-mut_g+1}^t \delta_{g,t,s}^{SU} \leq U_{g,t,s} \quad \forall g, \forall t \geq mut_g \quad (19)$$

$$\sum_{h=t-mdt_g+1}^t \delta_{g,t,s}^{SD} \leq 1 - U_{g,t,s} \quad \forall g, \forall t \geq mdt_g \quad (20)$$

Eq. (15) establishes the minimum and maximum output power limits for each generator. Ramp up/down limitation of output power is stated in Eq. (16). As described in Eqs. (17) and (18), the start-up and shutdown status of each generator is determined based on the production power of the generator in two consecutive hours. The minimum on/off time of the generators is also considered in the Eqs. (19) and (20) [31].

2.4. ESS operation

In [20], BESS technologies are categorized based on electrodes and electrolytes, with lead acid (Pb-Acid), nickel-cadmium (NiCd), lithium-ion (Li-ion), and sodium sulfur (NaS), due to their high power and energy density, fast response time, and efficiency. The BESS degradation is influenced by factors such as Depth of Discharge (DoD) per cycle and the number of charging/discharging cycles. Each BESS technology has a relationship between DoD and expected lifetime cycles. Fig. 2-a illustrates the approximation of the relationship between DoD and cycles using a piecewise linear approximation technique. The lifecycle degradation parameter for BESS technology at different DoD segments is defined in Eq. (21). This parameter quantifies the degradation or loss of performance that occurs over the lifespan of the BESS as a result of cycling and operating at specific DoD [20]:

$$\mu_{i,d} = \frac{N_{i,d}}{N_{i,\max}} \quad (21)$$

In the case of the considered battery, the parameter $\mu_{i,d}$ will have a value of 1 if the battery is selected to operate at the maximum DoD. This indicates the maximum degradation or loss of performance when the battery is operated at its maximum DoD. However, if the battery is performed at a lower DoD level, the parameter $\mu_{i,d}$ will have a value greater than 1.

The number of charging/discharging cycles of the battery during the planning period is determined in Eqs. (22) and (23).

$$\psi_{i,t,s} = [z_{i,t,s} - z_{i,t-1,s}] z_{i,t,s} \quad (22)$$

$$80. \sum_t \sum_s \psi_{i,t,s} \leq \frac{1}{TL} \sum_{d \in D} N_{i,D^{\max}} \mu_{i,d} \omega_{i,d} \quad (23)$$

According to the charging/discharging state of the BESS in two consecutive hours, the time of starting the battery charging mode is determined in Eq. (23). A crucial factor to consider when using batteries is the impact of DoD on their lifecycle. As the DoD in each cycle increases, the life cycle of the battery decreases. In Eq. (24), the total number of BESS cycles over the project lifetime is calculated. It is crucial to ensure that the calculated number of cycles does not surpass the predetermined lifecycle associated with the selected maximum DoD. Consequently, the installed BESS does not need to be replaced during the project's lifetime.

Due to the linearity of the proposed model, the linear piecewise approximation method has been used as shown in Fig. 2-b [20]. To linearize the BESS lifecycle, it is assumed that the curve representing the relationship between battery DoD and its lifecycle is divided into D segments.

The technical limitations related to the charging/discharging power and SoC of the BESS are given in Eqs. (24) to (29).

$$0 \leq Pch_{i,t,s}^B \leq P_i^B (1 - z_{i,t,s}) \quad \forall i, t \quad (24)$$

$$0 \leq Pdc_{i,t,s}^B \leq P_i^B z_{i,t,s} \quad \forall i, t \quad (25)$$

$$\chi_i^{\min} P_i^B \leq E_i^B \leq \chi_i^{\max} P_i^B \quad \forall i \quad (26)$$

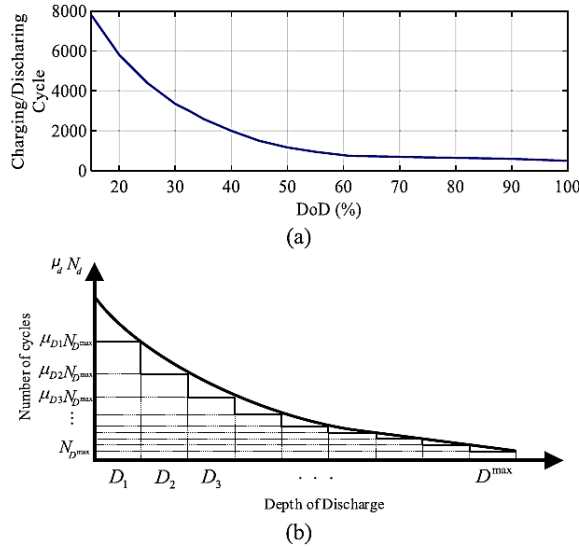


Fig. 2. BESS life cycle versus DoD. (a) NiCd battery. (b) Linearization of the BESS number of cycles versus DoD [20].

$$SOC_{i,t,s} = \left(1 - \sum_{d \in D} \xi_{i,d} \omega_{i,d}\right) E_i^B + \eta^{ch} \cdot Pch_{i,t,s}^B - \frac{Pdc_{i,t,s}^B}{\eta^{dch}} \quad \forall t = 1 \quad (27)$$

$$SOC_{i,t,s} = SOC_{i,t-1,s} + \eta^{ch} \cdot Pch_{i,t,s}^B - \frac{Pdc_{i,t,s}^B}{\eta^{dch}} \quad \forall t > 1 \quad (28)$$

$$\left(1 - \sum_{d \in D} \xi_{i,d} \omega_{i,d}\right) E_i^B \leq SOC_{i,t,s} \leq E_i^B \quad (29)$$

Each battery technology has a specific rated power that affects the charging and discharging of the BESS. Constraints Eqs. (24) and (25) limit the charging and discharging power of the battery to their rated power. If the binary variable Z is zero, the battery is charging, and if it is one, the battery is discharging. Therefore, according to these two relations, the battery cannot be charged and discharged simultaneously. There are practical limits to the ratio of the rated value of battery energy to its rated power. This limit is stated in Eq. (26), taking into account the ratio of conversion of energy to power. The SoC of the battery in the first hour and subsequent hours is expressed in Eqs. (27) and (28), respectively. The assumption is made that the battery begins operating at time t=1 with a complete discharge. According to Eq. (29), the battery SOC should not be less than a minimum value, and it should not exceed its capacity.

2.5. Information gap decision theory

Risk-averse strategies are impacted negatively by the uncertainty associated with specific parameters, which leads to an unfavorable effect on the problem's objective function. Put simply, when the uncertain parameter is realized, it can potentially increase the objective function from its baseline value. This is why the risk-averse strategy aims to determine the maximum range of uncertainty parameters that would result in the worst-case scenario for the objective function. This implies that the decision variables are optimized to attain the highest feasible uncertainty range for the uncertain parameter, while ensuring a specific increase in the objective function. All equations are based on a state without uncertainty and are equivalent to their predicted values. In line with the risk-averse (RA) strategy, reducing the output power of PV cells from their predicted values alters the objective function. In essence, the goal is to determine the maximum possible enlargement of the uncertainty range, while ensuring that the objective function does not exceed a predetermined limit. The parameter β represents the extent to which the objective function can be increased concerning its baseline value, considering undesirable uncertainties. The IGDT-based risk-averse strategy should be used as follows [32, 33]:

$$\max \alpha \quad \text{subject to (1) - (30)} \quad (30)$$

$$OF_1 \leq OF_1^{base} \cdot (1 + \beta) \quad (31)$$

$$G_{t,s}^{pv} = (1 - \alpha) \cdot \hat{G}_{t,s}^{pv} \quad (32)$$

The objective function, which aims to determine the maximum uncertainty radius, is expressed in Eq. (30). According to Eq. (31), the ship owner is willing to allocate a certain percentage, denoted as β , in addition to the target budget. This additional allocation is intended to ensure robust decision-making in light of uncertainties associated with the prediction of solar power. So, the value of β is determined by the decision-maker and represents their desired level of robustness for uncertainties in the prediction of solar power. It allows the decision-maker to account for and mitigate the potential risks and uncertainties associated with solar power predictions when making decisions. Indeed, it is worth noting that to calculate the baseline objective function (OF^{base}), the problem needs to be solved initially using the predicted values without considering the uncertainty in the solar power prediction. According to the radius of uncertainty, the range of solar power compared to the predicted value is specified in Eq. (32).

2.6. Linearization of the proposed model

By defining solar irradiation G^{PV} as an integer variable in the risk-averse strategy, Eq. (13) has become nonlinear due to the multiplication of two real variables. Therefore, the proposed method in [34] has been used to linearize the Eq. (13) as follows:

$$\underline{G}^{pv} + \sum_{o=1}^{N_O} (x_{t,s,o} \cdot \Delta G) \leq G_{t,s}^{pv} \leq \underline{G}^{pv} + \Delta G + \sum_{o=1}^O (x_{t,s,o} \cdot \Delta G) \quad (33)$$

$$\Delta G = \frac{\bar{G}^{pv} - \underline{G}^{pv}}{O + 1} \quad (34)$$

$$x_{t,s,o+1} \leq x_{t,s,o} \quad (35)$$

$$0 \leq \Delta G \cdot P^{ins} - pc_{t,s,o} \leq \Delta G \cdot \bar{P}^{ins} \cdot (1 - x_{t,s,o}) \quad (36)$$

$$0 \leq pc_{t,s,o} \leq \Delta G \cdot \bar{P}^{ins} \cdot x_{t,s,o} \quad (37)$$

$$P_{t,s}^{pv} = \left[(\underline{G}^{pv} + 0.5\Delta G) \cdot P^{ins} + \sum_{o=1}^O pc_{t,s,o} \right] \eta^{pv} \quad (38)$$

According to the value G^{PV} , the value of the binary variable $x_{t,s,o}$ is determined in each section. This constraint is expressed in Eq. (33). The discretization step of real integer G^{PV} is specified in Eq. (34). According to Eq. (35) to (37), the correction power $pc_{t,s,o}$ is determined. Finally, the linearized equation is stated in Eq. (38).

2.7. Epsilon-constraint method

In multi-objective problems, where there are multiple conflicting objectives, the aim is not to find a single solution but rather a set of optimal solutions or the Pareto front. The Pareto front represents a set of solutions where improving one objective comes at the cost of worsening another. These solutions are considered non-dominated, meaning that no other solution in the set can improve on at least one objective without sacrificing another. The Pareto front provides decision-makers with a range of options that trade-off different objectives and allows them to make informed decisions based on their preferences and priorities. The epsilon constraint method is one of the common algorithms for solving the multi-objective optimization problem. One of the advantages of the epsilon constraint method is that, unlike the weighting method, the number of generated solutions can be easily controlled by adjusting the number of domain divisions of each objective function [35]. In the epsilon constraint method, the second objective function is defined as the inequality constraint of the optimization problem, and by gradually decreasing the epsilon value; the results are obtained as Pareto optimal solutions. Therefore, Eq. (39) determines the range of the second objective function as a constraint in the optimization problem.

$$OF_2 \leq OF_2^{\max} - \varepsilon \left(\frac{OF_2^{\max} - OF_2^{\min}}{N - 1} \right) \quad (39)$$

Then, according to Eq. (40), by applying the fuzzy method, fuzzy values between [0, 1] are assigned to each objective function for each Pareto solution.

$$\mu_j(X) = \frac{OF_j^{\max} - OF_j(X)}{OF_j^{\max} - OF_j^{\min}} \quad (40)$$

Finally, by specifying the weighting coefficients for each objective function by the designer, the desired optimal solution is determined using the Minimax optimization method according to Eq. (41).

$$\min_X (\max_j |W_j - \mu_j(X)|) \quad (41)$$

3. SIMULATION RESULTS

The studied ship power system has two diesel generators and the technical parameters of the generators are presented in Table 1 [36]. The available area of the ship's deck for installing PV cells is approximately $100m^2$. This area serves as the available space for placing the photovoltaic panels to capture solar energy. The hourly solar irradiation on a warmest day is presented in Fig. 3 [9]. Also, Fig. 4 illustrates the solar radiation correction coefficient for different seasons. Each m^2 of PV cell can produce a maximum power of 1.1 kW. The required information about PV cells is given in the Table 2.

In this article, BESS technology is classified into four groups: Pb-Acid, NiCd, Li-ion, and NaS, which the technology specifications of Each battery, and the points corresponding to the battery life cycle reduction curve are illustrated in Tables 3 and 4 respectively [20, 37, 38]. Fig. 5 depicts the hourly load profile along the route [21].

The Investment planning is made for 15 years. In the analysis, an assumption is made that the interest rate is 4%. The interest rate is a crucial parameter used to calculate various financial aspects of the hybrid ship power system. The linearization steps for the quadratic cost and pollution functions as well as the linearization of the product of two real variables in IGDT-based strategy have been considered equal to 10. Increasing the linearization steps gives a more accurate response, but also increases the simulation time.

Table 1. Technical parameters for diesel generators.

| Generator | $P^{min}(MW)$ | $P^{max}(MW)$ | mut(h) | mdt(h) |
|-----------|--------------------|-----------------|----------------|-----------|
| G1 | 0.03 | 0.20 | 2 | 2 |
| G2 | 0.05 | 0.20 | 2 | 2 |
| Generator | $a(\$/MWh^2)$ | $b(\$/MWh)$ | $c(\$/h)$ | C^{CSU} |
| G1 | 0.0048 | 16.19 | 1000 | 9000 |
| G2 | 0.0020 | 16.50 | 680 | 1120 |
| Generator | $\alpha(kg/MWh^2)$ | $\beta(kg/MWh)$ | $\gamma(kg/h)$ | C^{HSU} |
| G1 | 0.003 | -0.244 | 10.34 | 4500 |
| G2 | 0.005 | -0.406 | 30.03 | 560 |

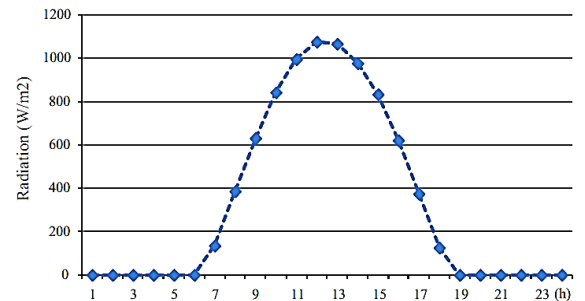


Fig. 3. Solar radiation on the warmest day [20].

To confirm the efficiency of the proposed model, four different case studies have been investigated as follows:

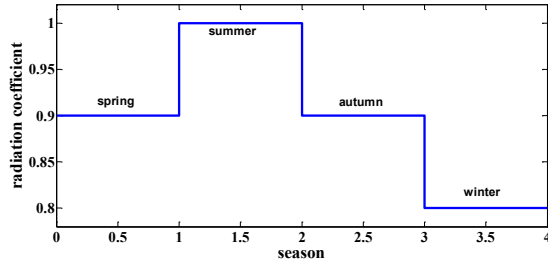


Fig. 4. Solar irradiation correction coefficient.

Table 2. PV data.

| Parameter | Value | Parameter | Value |
|--------------------|------------|-------------------|------------|
| Lifetime | 15 yrs. | Efficiency | 95% |
| Investment cost | 1800 \$/kW | Replacement cost | 1800 \$/kW |
| Length of PV panel | 1.66 m | Width of PV panel | 0.99 m |

Case 1: considering the diesel generator only.

Case 2: deterministic strategy considering the diesel generator, PV, and ESS.

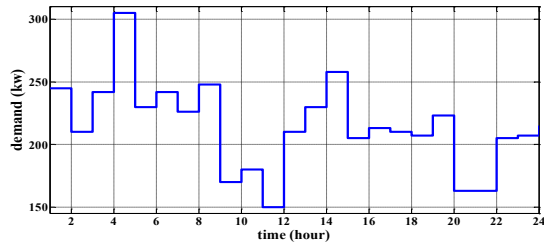


Fig. 5. Ship load profile along the route.

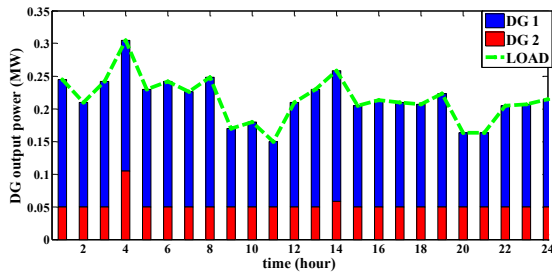


Fig. 6. The output power of generators in case 1.

Case 3: IGDT-based strategy considering the diesel generator, PV, and ESS.

Case 4: Multi-objective optimization considering cost and CO_2 emissions.

The MILP problem, taking into account the assumptions mentioned above, is implemented in GAMS software and solved utilizing the CPLEX solver on a PC equipped with an Intel Core processor running at 4 GHz and having 32 GB of RAM.

Case 1: In this case, where PV cells and batteries are not utilized, 25,882,843\$ has been spent on supplying the electrical energy needed by the ship power system. Also, the amount of 309,650 tons of pollution has been emission by generators yearly. The active power produced by generators is shown in Fig. 6. Due to the high start-up cost of the generators, both generators are on all day long. Also, the main part of the load is provided by generator 1, which has a lower cost, and during many hours of the day, generator 2 works with lowest power.

Table 3. BESS technologies characteristics.

| Parameter | Pb-Acid | NiCd | NaS | Li-ion |
|--------------------------------|---------|------|------|--------|
| Power investment cost (\$/kW) | 200 | 400 | 300 | 300 |
| Energy investment cost (\$/kW) | 200 | 474 | 350 | 695 |
| O and M cost (\$/kW/year) | 50 | 20 | 80 | - |
| Installation cost (\$/kW) | 20 | 12 | 8 | 3.6 |
| $\eta(\%)$ | 70 | 85 | 95 | 98 |
| χ_{min}, χ_{max} | 1, 8 | 1, 8 | 1, 6 | 1, 8 |
| $T_B(\text{years})$ | 12 | 20 | 20 | 20 |
| N_{max} | 550 | 500 | 2500 | 3000 |

Table 4. BESS lifecycle reduction data.

| DoD (%) | Pb-Acid | NiCd | NaS | Li-ion |
|---------|---------|------|------|--------|
| 10 | 6.9 | 15.8 | 17.2 | - |
| 20 | 5.2 | 11.6 | 8.8 | - |
| 30 | 3.7 | 6.8 | 5.8 | - |
| 40 | 2.4 | 4.0 | 4.3 | - |
| 50 | 1.9 | 2.4 | 3.4 | 2.7 |
| 60 | 1.6 | 1.8 | 2.8 | 2.3 |
| 70 | 1.4 | 1.6 | 2.6 | 1.9 |
| 80 | 1.2 | 1.4 | 2.2 | 1.5 |
| 90 | 1.1 | 1.2 | 1.8 | 1.2 |
| 100 | 1.0 | 1.0 | 1.0 | 1.0 |

Case 2: In the second case, there is the possibility of installing solar cells and energy storage batteries. This option allows for the generation of electrical energy through solar power and the ability to store excess energy for later use. It should also be noted that in this case, no uncertainty is considered for solar radiation; but the change of solar radiation in different seasons is considered as shown in Fig. 4.

In this case, by installing solar cells in the available area of the ship, the maximum possibility of producing 97.3 kW of solar power has been provided. Also, three models of Pb-acid, NaS, and Li-ion batteries are used with an investment cost of 31,510\$, the specifications of which are given in Table 5.

Table 5. Specifications of the installed battery in case 2.

| Parameter | Pb-Acid | NaS | Li-ion |
|--------------------|---------|-------|--------|
| Rated power (kW) | 5.3 | 207.0 | 123.7 |
| Rated energy (kWh) | 22.6 | 773.7 | 346.3 |
| Maximum DoD (%) | 40 | 80 | 70 |
| Number of cycles | 80 | 320 | 320 |
| Initial SoC (kWh) | 13.6 | 154.7 | 103.9 |

The SoC of NaS and Li-ion batteries during 24 hours in the spring season are shown in Fig. 7. The output power of each generator is also shown in Fig. 8. First, generator 1 starts working with maximum power and then turns off at 3 o'clock. From 3 o'clock, generator 2 is turned on as an alternative and starts producing energy with maximum power. The details of investment costs and the amount of pollutants are also specified in Table 6. In total, with the installation of solar cells and batteries, the cost has been determined at 18,291,373\$, which has decreased by 23% compared to case 1. Also, with the emission of 207,919 tons of pollutants, the emission of pollutants has also reduced by 33% compared to case 1. This significant reduction in costs and emissions proves the necessity of simultaneously using renewable resources and batteries in a ship's power system.

Case 3: In this case, the uncertainty in the solar radiation and as a result the uncertainty in the production power of solar cells is also taken into account, but there is no accurate information about the amount of prediction error. Regardless of the uncertainty, the installation decision of batteries and solar cells may not be correct and may lead to an increase in costs.

In IGDT based decision-making method, the decision-maker is willing to increase the investment budget to overcome the wrong decision in case of deviation from the predicted value and make a robust decision. According to the amount of cost of 18,291,397\$ in case 2, the decision-maker is willing to increase the investment budget to the amount of 18,500,000\$ (only 1.1% increase in the budget).

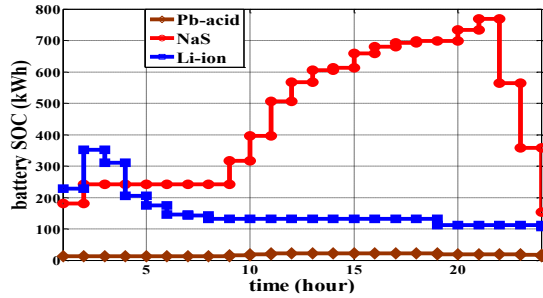


Fig. 7. Battery SoC in case 2.

Table 6. Cost and emission in case 2.

| | Diesel generator cost (\$) | PV investment cost (\$) | Battery investment cost (\$) | Emission (ton) |
|------------------------|----------------------------|-------------------------|------------------------------|----------------|
| | 18,187,050 | 31,510 | 72,815 | 207,919 |
| Total cost (\$) | 18,291,373 | | | |

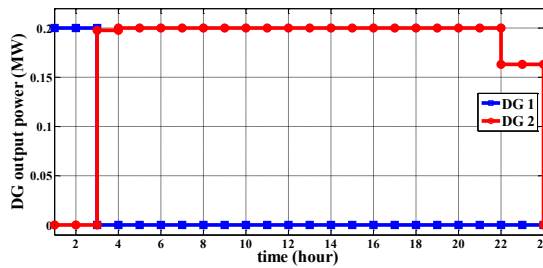


Fig. 8. The output power of diesel generators in the case 2.

Table 7. Specifications of the installed battery in case 3.

| Parameter | Pb-Acid | NaS | Li-ion |
|--------------------|---------|-------|--------|
| Rated power (kW) | 3.5 | 206.3 | 143.8 |
| Rated energy (kWh) | 28.2 | 522 | 402.8 |
| Maximum DoD (%) | 40 | 80 | 70 |
| Number of cycles | 80 | 320 | 320 |
| Initial SoC (kWh) | 16.9 | 104.4 | 120.8 |

In this case, by incorporating solar cells and energy storage batteries, it is possible to achieve a maximum radius of uncertainty of 0.19, while only increasing the investment budget by 1.1%. This indicates that with a relatively small increase in the budget, the ship's power system can be made more robust and resilient to uncertainties in solar power predictions. Taking into account the uncertainty in solar power, it has been determined that 78 kW of solar cells will be installed on the ship's deck. This installation represents a decrease of 20% compared to Case 2, where the

Table 8. Cost and emission in case 3.

| | Diesel generator cost (\$) | PV investment cost (\$) | Battery investment cost (\$) | Emission (ton) |
|------------------------|----------------------------|-------------------------|------------------------------|----------------|
| | 18,405,840 | 25,236 | 68,681 | 217,502 |
| Total cost (\$) | 18,499,758 | | | |

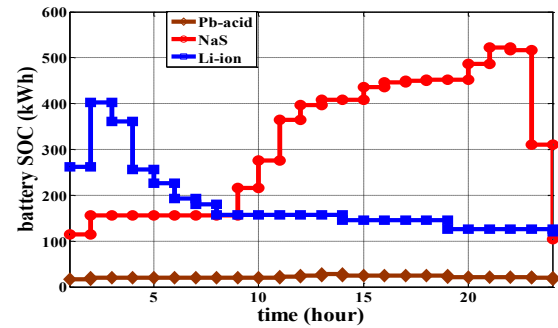


Fig. 9. Battery SoC in case 3 (spring season).

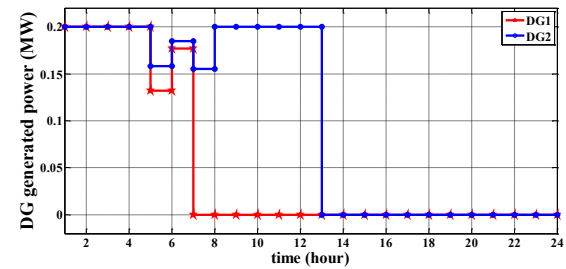


Fig. 10. Diesel generators output power in case 3.

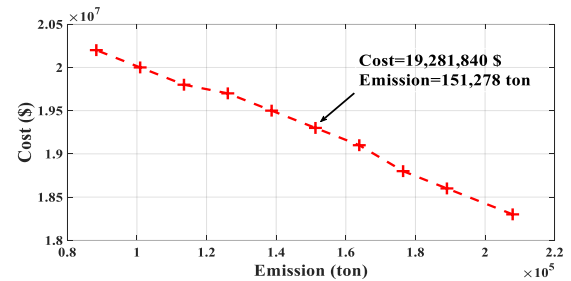


Fig. 11. Pareto front in case 4.

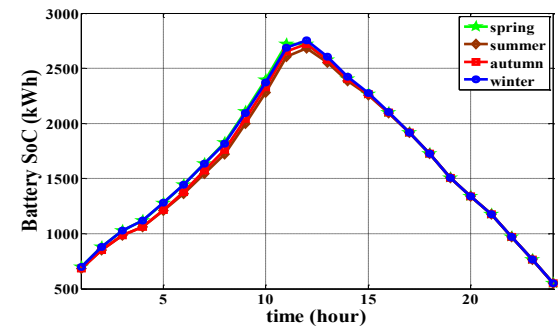


Fig. 12. NaS battery SoC in case 4.

uncertainty was not considered. The reduction in the installed capacity accounts for the potential variations and uncertainties in solar power generation, ensuring that the system remains efficient and effective even under uncertain conditions. Also, three types of

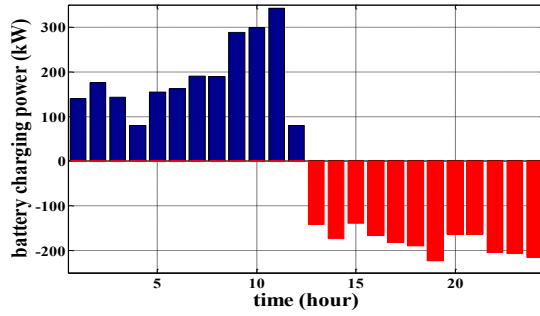


Fig. 13. Charging/discharging power of the battery in case 4.

Table 9. Specifications of the installed battery in case 4.

| Parameter | NaS |
|--------------------|--------|
| Rated power (kW) | 459.2 |
| Rated energy (kWh) | 2755.3 |
| Maximum DoD (%) | 80 |
| Number of cycles | 320 |
| Initial SoC (kWh) | 551 |

Pb-acid, Li-ion, and NaS batteries are used in IGDT based strategy and their specifications are given in Table 7. The SoC of the installed batteries during 24 hours in the spring season is shown in Fig. 9. The diesel generator's production power scheduling is also shown in Fig. 10.

With the equipment installed on the ship and the specified schedule for the generated power of the diesel generators and charging/ discharging of the batteries, the details of the costs and the amount of emissions are given in Table 8. Considering the uncertainty in solar production power and referring to Table 8, it is observed that there is a 20% decrease in the investment in solar cell installation and a 6% decrease in the investment in battery installation compared to Case 2. This decrease in investment in renewable sources and batteries has led to a 1.2% increase in diesel generators' energy production cost, and as a result, a 4.6% increase in pollution compared to case 2.

Case 4: In this case, the objective function takes into account the simultaneous consideration of minimizing both the cost and the amount of pollution. By incorporating both goals in the objective function, the optimization process aims to find a solution that achieves a balance between minimizing costs associated with the energy system and reducing the environmental impact in terms of pollution. This approach allows for a comprehensive evaluation and decision-making process that considers both economic and environmental aspects simultaneously. By implementing the proposed model, the Pareto front is shown in Fig. 11. By implementing the proposed model, the Pareto front is depicted in Fig. 11. To make an optimal decision, the decision-maker needs to determine the fuzzy coefficient for each function. The fuzzy coefficients reflect the decision-maker's preferences and priorities, allowing them to assign weights or importance to different objectives in the multi-objective optimization problem. Here, the fuzzy coefficient of cost and pollution minimization is taken to 0.8 and 0.7, respectively.

Using the fuzzy method, the optimal answer is specified in Fig. 11. At this particular point on the Pareto front, the amount of cost is equal to 19,281,840\$ while the amount of pollutants is equal to 151,278 tons. The optimal decision at this point includes installing 109.9 kW of solar cells. In this case, one type of NaS battery should be installed; their specifications are given in Table 9. The SOC of the NaS battery in all four seasons is shown in Fig. 12. According to Fig. 12, the SOC of the NaS battery in four seasons does not differ much from each other. Based on the given information, it can be inferred that the charging/discharging

Table 10. Cost and emission in case 4.

| Diesel generator cost (\$) | PV investment cost (\$) | Battery investment cost (\$) | Emission (ton) |
|----------------------------|-------------------------|------------------------------|----------------|
| 19,108,420 | 35,574 | 137,845 | 151,278 |
| Total cost (\$) | | 19,281,840 | |

schedule of the battery will remain relatively consistent across different seasons. This implies that the battery's operation and energy management strategy are designed to be seasonally robust, resulting in a similar charging and discharging pattern throughout the year. In this case, the battery is continuously charged until 12:00 and then fully discharged until 24:00. Scheduling of battery charging/discharging is shown in Fig. 13. Positive values indicate charge power and negative values indicate discharge power.

The daily power schedule of the diesel generators in summer is shown in Fig. 10. The details of the costs and the amount of pollution at the optimal point are specified in Table 10.

4. FUTURE STUDIES

In this article, a 24-hour radiation curve is used to consider solar radiation, which of course changes with a coefficient according to different seasons. However, a ship sailing in the oceans and open seas will be present in different geographical locations throughout the year, so it would be ideal if, considering the characteristics of the ship's journey throughout the year and its presence in different geographical locations, the solar radiation was calculated at each point of the route and the optimization problem was solved dynamically. Of course, it should be noted that in this case, the dimensions of the problem would also become larger and the use of the GAMS software and the Cplex solver would require a long time. Therefore, it is suggested that in this case, metaheuristic algorithms such as NSGA-II or MOPSO be used to solve the problem.

5. CONCLUSION

In this article, a Mixed-Integer Linear Programming model is proposed for the optimal planning and scheduling of a hybrid ship power system. Investment options include solar power systems and four different battery technologies. The model is formulated based on two objective functions: cost minimization and emission minimization. Due to the conflicting nature of these objectives, the ε -constraint method and fuzzy decision-making have been employed to determine the optimal investment plan. To account for the uncertainty in solar power prediction, the Information Gap Decision Theory (IGDT) method is also utilized. To evaluate the proposed model, four different case studies have been analyzed. In the first case, using only diesel generators to meet the ship's power demand results in a total cost of \$25,882,843 and 309,650 tons of emissions. In the second case, by optimally selecting the power capacity and technology for installing solar PV and batteries, costs and emissions are reduced by 23% and 33%, respectively, compared to the first case. In the third case, using the IGDT method, an increase of only 1.1% in the investment budget makes the decision robust to a 19% error in solar power prediction. In this scenario, with reduced investment in solar panels and batteries, diesel generators play a larger role in supplying the ship's load, leading to a 4.6% increase in emissions compared to the second case. Finally, in the fourth case, considering both cost and emission minimization, fuzzy coefficients of 0.8 and 0.7 are assigned to the two objective functions, respectively. As a result, the optimal investment and scheduling plan is determined, leading to a 5.4% increase in cost but a 27% reduction in emissions compared to the second case.

REFERENCES

- [1] S. Alessandro, P. Mario, and D. Alfonso, "A novel highly integrated hybrid energy storage system for electric propulsion and smart grid applications," in *Adv. Energy Storage Technol.* (C. Xiangping and C. Wenping, eds.), p. Ch. 4, Rijeka: IntechOpen, 2018.
- [2] Z. Jin *et al.*, "Hierarchical control design for a shipboard power system with dc distribution and energy storage aboard future more-electric ships," *IEEE Trans. Ind. Inf.*, vol. 14, no. 2, pp. 703–714, 2018.
- [3] H. Jabari *et al.*, "A review on propulsion drive trains of electric ships: Structures, challenges and opportunities," *J. Energy Manage. Technol.*, vol. 9, no. 1, pp. 1–13, 2025.
- [4] I. Atawi *et al.*, "Recent advances in hybrid energy storage system integrated renewable power generation: Configuration, control, applications, and future directions," *Batteries*, vol. 9, no. 1, p. 29, 2023.
- [5] R. Iqbal *et al.*, "Comparative study based on techno-economics analysis of different shipboard microgrid systems comprising pv/wind/fuel cell/battery/diesel generator with two battery technologies: A step toward green maritime transportation," *Renew. Energy*, vol. 221, p. 119670, 2024.
- [6] A. Dolatabadi, R. Ebadi, and B. Mohammadi-Ivatloo, "A two-stage stochastic programming model for the optimal sizing of hybrid pv/diesel/battery in hybrid electric ship system," *J. Oper. Autom. Power Eng.*, vol. 7, no. 1, pp. 16–26, 2019.
- [7] C. Leone *et al.*, "Multi-objective optimization of pv and energy storage systems for ultra-fast charging stations," *IEEE Access*, vol. 10, pp. 14208–14224, 2022.
- [8] A. El Shamy, P. Aduama, and A. Al-Sumaiti, "Chance constrained optimal sizing of a hybrid pv/battery/hydrogen isolated microgrid: A life-cycle analysis," *Energy Convers. Manage.*, vol. 332, p. 119707, 2025.
- [9] X. Bao *et al.*, "Optimal sizing of battery energy storage system in a shipboard power system with considering energy management optimization," *Discrete Dyn. Nat. Soc.*, vol. 2021, p. 9032206, 2021.
- [10] C. Chen *et al.*, "Optimal allocation and economic analysis of energy storage system in microgrids," *IEEE Trans. Power Electron.*, vol. 26, no. 10, pp. 2762–2773, 2011.
- [11] N. Bigdeli, "Optimal management of hybrid pv/fuel cell/battery power system: A comparison of optimal hybrid approaches," *Renew. Sustain. Energy Rev.*, vol. 42, pp. 377–393, 2015.
- [12] P. Zhao, J. Wang, and Y. Dai, "Capacity allocation of a hybrid energy storage system for power system peak shaving at high wind power penetration level," *Renew. Energy*, vol. 75, pp. 541–549, 2015.
- [13] M. Arifujjaman, "A comprehensive power loss, efficiency, reliability and cost calculation of a 1 mw/500 kwh battery based energy storage system for frequency regulation application," *Renew. Energy*, vol. 74, pp. 158–169, 2015.
- [14] H. Zhao *et al.*, "Review of energy storage system for wind power integration support," *Appl. Energy*, vol. 137, pp. 545–553, 2015.
- [15] A. Boveri *et al.*, "Optimal sizing of energy storage systems for shipboard applications," *IEEE Trans. Energy Convers.*, vol. 34, no. 2, pp. 801–811, 2018.
- [16] A. Bukar *et al.*, "Optimal planning of hybrid photovoltaic/battery/diesel generator in ship power system," *Int. J. Power Electron. Drive Syst.*, vol. 11, p. 1527, 2020.
- [17] A. Diab *et al.*, "Application of different optimization algorithms for optimal sizing of pv/wind/diesel/battery storage stand-alone hybrid microgrid," *IEEE Access*, vol. 7, pp. 119223–119245, 2019.
- [18] A. Mohammed *et al.*, "Review of optimal sizing and power management strategies for fuel cell/battery/super capacitor hybrid electric vehicles," *Energy Rep.*, vol. 9, pp. 2213–2228, 2023.
- [19] H. Akter *et al.*, "A short assessment of renewable energy for optimal sizing of 100% renewable energy based microgrids in remote islands of developing countries: A case study in bangladesh," *Energies*, vol. 15, no. 3, p. 1084, 2022.
- [20] M. Moradzadeh and M. Abdelaziz, "A new milp formulation for renewables and energy storage integration in fast charging stations," *IEEE Trans. Transp. Electr.*, vol. 6, no. 1, pp. 181–198, 2020.
- [21] H. Lan *et al.*, "Optimal sizing of hybrid pv/diesel/battery in ship power system," *Appl. Energy*, vol. 158, pp. 26–34, 2015.
- [22] H. Liu *et al.*, "Estimation of pv output power in moving and rocking hybrid energy marine ships," *Appl. Energy*, vol. 204, pp. 362–372, 2017.
- [23] A. Sari *et al.*, "New optimized configuration for a hybrid pv/diesel/battery system based on coyote optimization algorithm: A case study for hotan county," *Energy Rep.*, vol. 8, pp. 15480–15492, 2022.
- [24] J. Zhu *et al.*, "Bi-level optimal sizing and energy management of hybrid electric propulsion systems," *Appl. Energy*, vol. 260, p. 114134, 2020.
- [25] H. Chen *et al.*, "Optimization of sizing and frequency control in battery/supercapacitor hybrid energy storage system for fuel cell ship," *Energy*, vol. 197, p. 117285, 2020.
- [26] C. Yao, M. Chen, and Y. Hong, "Novel adaptive multi-clustering algorithm-based optimal ess sizing in ship power system considering uncertainty," *IEEE Trans. Power Syst.*, vol. 33, no. 1, pp. 307–316, 2018.
- [27] W. Cao, P. Geng, and X. Xu, "Optimization of battery energy storage system size and power allocation strategy for fuel cell ship," *Energy Sci. Eng.*, vol. 11, no. 6, pp. 2110–2121, 2023.
- [28] P. Venkatesh, R. Gnanadass, and N. Padhy, "Comparison and application of evolutionary programming techniques to combined economic emission dispatch with line flow constraints," *IEEE Trans. Power Syst.*, vol. 18, no. 2, pp. 688–697, 2003.
- [29] N. Kumar, S. Dahiya, and K. Parmar, "Sensitivity analysis based multi-objective economic emission dispatch in microgrid," *J. Oper. Autom. Power Eng.*, vol. 13, no. 2, pp. 127–139, 2025.
- [30] N. Kumar, S. Dahiya, and K. Parmar, "Multi-objective economic emission dispatch optimization strategy considering battery energy storage system in islanded microgrid," *J. Oper. Autom. Power Eng.*, vol. 12, no. 4, pp. 296–311, 2024.
- [31] M. Alizadeh, M. Jafari, and G. Karami, "Mixed integer linear programming for thermal units unit commitment considering load uncertainty, renewable resources and electric vehicles," *Nonlinear Syst. Electr. Eng.*, vol. 7, no. 1, pp. 108–130, 2020.
- [32] F. Jabari *et al.*, "Introduction to information gap decision theory method," in *Robust Opt. Plan. Oper. Electr. Energy Syst.*, pp. 1–10, 2019.
- [33] F. Jabari *et al.*, "Robust unit commitment using information gap decision theory," in *Robust Opt. Plan. Oper. Electr. Energy Syst.*, pp. 79–93, 2019.
- [34] A. Rueda-Medina *et al.*, "A mixed-integer linear programming approach for optimal type, size and allocation of distributed generation in radial distribution systems," *Electr. Power Syst. Res.*, vol. 97, pp. 133–143, 2013.
- [35] M. Kiptoo *et al.*, "Optimal capacity and operational planning for renewable energy-based microgrid considering different demand-side management strategies," *Energies*, vol. 16, no. 10, p. 4147, 2023.
- [36] A. Shahmoradi and M. Kalantar, "Resource scheduling in a smart grid with renewable energy resources and plug-in vehicles by minlp method," *AUT J. Electr. Eng.*, vol. 47, no. 2, pp. 39–47, 2015.
- [37] D. Akinyele, J. Belikov, and Y. Levron, "Battery storage technologies for electrical applications: Impact in stand-alone photovoltaic systems," *Energies*, vol. 10, no. 11, p. 1760, 2017.

- [38] X. Luo *et al.*, “Overview of current development in electrical energy storage technologies and the application potential in power system operation,” *Appl. Energy*, vol. 137, pp. 511–536, 2015.